Numerical Investigation of Complex, Transitional, and Chemically Reacting Flows

S.-W. Kim
Resident Research Associate
NASA Lewis Research Center
Cleveland, Ohio 44135

Part A. On Turbulent Transport of chemical Species in Compressible Reacting Flows

Contents

Mixing of chemical species in reacting flows

Chemically Reacting Laminar Flows

Numerical (or semi-analytical) methods

O.D.E. solvers
1-D Numerical methods
Numerical uncertainty is minimal

Chemical kinetics

Chemical kinetics (finite rate chemical kinetics & Reduced finite rate chemical kinetics) for certain fuels (hydrogen and some of hydro-carbons) have been tested and validated repeatedly.

Numerical and theoretical analyses yield accurate results.

Chemically Reacting Turbulent Flows

Numerical methods

Boundary layer or Navier-Stokes equations solvers
(Except for semi-analytical analyses of PSR cases)

Uncertainty is caused partly by numerical methods.

Chemical kinetics

Finite rate chemical kinetics & Reduced finite rate chemical are used.

Uncertainty is caused partly by over-simplified chemical kinetics.

Turbulence Equations

Numerical analysis yields not so accurate results. Unceratinlty caused by turbulence equations is by far greater than that caused by chemical kinetics.*

The probability density functions are used to improve the predictive capability of turbulent mixing of chemical species. However, some pdf methods yield physically incorrect numerical results.

It is certainly important to better understand the turbulent mixing of chemical species in reacting flows.

*Westbrook and Dryer, *Prog. Energy Combustion Science*, vol. 10, pp. 1-57, 1984.

Turbulent Mixing of Chemical Species in Reacting Flows

1. Large eddy mixing
2. Turbulent Mixing
3. Molecular Mixing

The use of accurate chemical kinetics alone can not yield accurate results for numerical analysis of turbulent reacting flows unless turbulent mixing is resolved correctly.

Large Eddy Mixing

Caused by separated flows, recirculating flows, and organized structures.

The extent of calculated recirculation zone or the organized structures depends on the accuracy of both the numerical method and the turbulence equations since they are nonlinearly coupled with each other.

$$\frac{\partial}{\partial t}(\rho u_i)+\frac{\partial}{\partial x_j}(\rho u_i u_j)-\frac{\partial}{\partial x_j}\left[(\mu+\mu_t)\left(\frac{\partial u_i}{\partial x_j}+\frac{\partial u_j}{\partial x_i}\right)\right]=-\frac{\partial p}{\partial x_i}$$

$$\frac{\partial}{\partial t}(\rho k)+\frac{\partial}{\partial x_j}(\rho u_j k)-\frac{\partial}{\partial x_j}\left[\left(\frac{\mu+\mu_t}{\sigma_t}\right)\frac{\partial k}{\partial x_j}\right]=P_r-\varepsilon_t$$

where $\mu_t = \mu_t(k, \varepsilon_t, \cdots)$, and $P_r=\frac{\mu_t}{\rho}\left[2\left(\frac{\partial u}{\partial x}\right)^2+2\left(\frac{\partial v}{\partial y}\right)^2+\left(\frac{\partial u}{\partial y}+\frac{\partial v}{\partial x}\right)^2\right]$

Therefore, the capability to correctly resolve the large eddy mixing depends on the accuracy of the numerical method and the turbulence equations.

Numerical investigations carried out during last decades show that k-ε, ARSM, and RSM do not yield accurate results for complex turbulent flows.

On the other hand, the multiple-time-scale turbulence equations* yield highly improved numerical results for various complex turbulent flows.

*Kim and Benson, *Int. J. Heat Mass Transfer*, vol.35, pp. 2357-2365, 1992.

Turbulent Mixing

Caused mostly by energy-containing eddies and partly by fine-scale eddies.

The capability to resolve the turbulent mixing of chemical species depends on the capability of the turbulence equations to correctly describe the turbulent transport of scalar variables (i.e., heat transfer, turbulent kinetic energy, concentrations, and convection-diffusion of species, etc)

Need to be able to describe the chemical reaction-turbulence interaction (i.e., turbulent mixing is enhanced and shear layer thickness is widened by chemical reaction)*

The multiple-time-scale turbulence equations can resolve the cascade of turbulent kinetic and the nonequilibrium turbulence phenomena.
(Present numerical results show that the M-S turbulence equations can resolve the chemical reaction-turbulence interaction.)

* C.T. Chang et al., "Comparison of reacting and non-reacting shear layers at a high subsonic mach number," AIAA paper 93-2381, 1993.

Molecular Mixing

Caused by molecular diffusivity.

Theoretical and numerical analyses of chemically reacting laminar flows yield accurate results.

Various molecular diffusion equations can accurately describe the molecular diffusion of species.

The Lennard-Jones 12-6 potential law is used in the present study.

Various numerical methods that yield accurate results for laminar flows can resolve the molecular mixing.

Multiple-time-scale turbulence equations

Energy containing eddies

$$\frac{\partial}{\partial t}(\rho k_p) + \frac{\partial}{\partial x_j}(\rho u_j k_p) - \frac{\partial}{\partial x_j}\left\{\left(\mu + \frac{\mu_t}{\sigma_{kp}}\right)\frac{\partial k_p}{\partial x_j}\right\} = \rho P_r - \rho \varepsilon_p$$

$$\frac{\partial}{\partial t}(\rho \varepsilon_p) + \frac{\partial}{\partial x_j}(\rho u_j \varepsilon_p) - \frac{\partial}{\partial x_j}\left\{\left(\mu + \frac{\mu_t}{\sigma_{\varepsilon p}}\right)\frac{\partial \varepsilon_p}{\partial x_j}\right\} = \frac{\rho}{k_p}(c_{p1}P_r^2 + c_{p2}P_r\varepsilon_p - c_{p3}\varepsilon_p^2)$$

Fine Scale Eddies

$$\frac{\partial}{\partial t}(\rho k_t) + \frac{\partial}{\partial x_j}(\rho u_j k_t) - \frac{\partial}{\partial x_j}\left\{\left(\mu + \frac{\mu_t}{\sigma_{kt}}\right)\frac{\partial k_t}{\partial x_j}\right\} = \rho \varepsilon_p - \rho \varepsilon_t$$

$$\frac{\partial}{\partial t}(\rho \varepsilon_t) + \frac{\partial}{\partial x_j}(\rho u_j \varepsilon_t) - \frac{\partial}{\partial x_j}\left\{\left(\mu + \frac{\mu_t}{\sigma_{\varepsilon t}}\right)\frac{\partial \varepsilon_t}{\partial x_j}\right\} = \frac{\rho}{k_t}(c_{t1}\varepsilon_p^2 + c_{t2}\varepsilon_p\varepsilon_t - c_{t3}\varepsilon_t^2)$$

Turbulent Eddy Viscosity

$$\mu_t = \rho c_\mu k^2/\varepsilon_p \text{ where } c_\mu = c_{\mu f}\varepsilon_t/\varepsilon_p$$

Remark: Single-time-scale turbulence models can not resolve nonequilibrium turbulence phenomena.

Species conservation equations for reacting flows

Chemical species concentration equation

$$\frac{\partial}{\partial t}(\rho Y_i) + \nabla \cdot \{\rho Y_i(v + V_i)\} = \dot{w}_i$$

where the diffusion velocity, V_i, is approximated using the Fick's law given as

$$Y_i V_i = -(D_{i,l} + D_{i,t})\nabla Y_i$$

The production rate of the *i*-th species, $\dot{w}_i$, is given as

$$\dot{w}_i = \sum_{k=1}^{N_r} M_i\left(n''_{i,k} - n'_{i,k}\right) w_k$$

where

$$\omega_k = k_{f,k}\prod_{j=1}^{N_s} c_j^{\nu'_{j,k}} - k_{b,k}\prod_{j=1}^{N_s} c_j^{\nu''_{j,k}}$$

Chemical reactions for the combustion of H_2 in a vitiated supersonic airstream are described using 9 chemical species (H_2, O_2, H_2O, OH, O, H, HO_2, H_2O_2, and N_2) and 24 pairs of reaction-steps (Burks and Oran, 1981; Kumar, 1989).

A fast chemistry can not be used to describe the fine details of chemically reacting flows.

A reduced chemical kinetics can not be used confidently due to the uncertainty contained in the reaction mechanisms.

The use of a detailed finite rate chemistry may make it difficult to obtain a fully converged solution due to the coupling between the large number of flow, turbulence, and chemical equations. The numerical method needs to be strongly convergent. Accuracy also depends on the capability of turbulence equations used.

Numerical Method

The numerical method is a finite volume method that incorporates a pressure-staggered mesh and an incremental pressure equation for the conservation of mass.

Predictor Step: Solve momentum equation.

$$(\rho C_1+A_i^*)u_i^{**}=\sum_{nb} A_k^* u_k^{**} + S_i^* - \frac{\partial p^*}{\partial x_i} + \rho C_2 u_i^{n-1} - \rho C_3 u_i^{n-2} \quad (1)$$

Corrector Step: Correct the velocity field to be divergence free

Incremental pressure equation

$$\frac{\partial}{\partial x_j}\left(\frac{p'}{RT}u_j^{**}\right) - \frac{\partial}{\partial x_j}\left[\frac{1}{(\rho C_1+A_j^*)}\frac{\partial p'}{\partial x_j}\right] = -\frac{\partial u_j^{**}}{\partial x_j} \quad (2)$$

Incremental velocity equation

$$u_i' = \frac{1}{(\rho C_1+A_i^*)}\frac{\partial p'}{\partial x_i} \quad (3)$$

Velocity and pressure corrections

$$u_i^{***} = u_i^{**} + u_i' \tag{4}$$

$$p^{**} = p^{*} + p' \tag{5}$$

Solve eqs. (1-5) iteratively until all flow variables are converged.

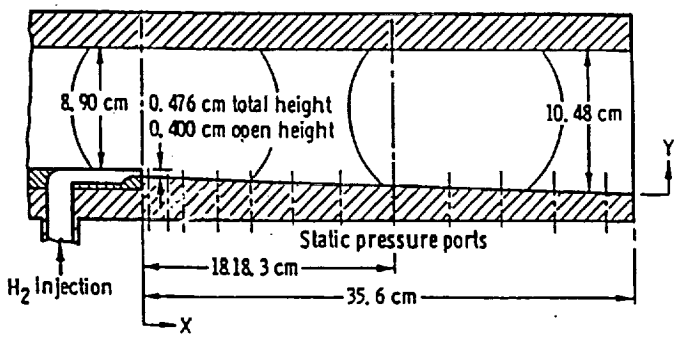

Combustion of H_2 in vitiated supersonic airstream (Burrows and Kurkov, 1973)

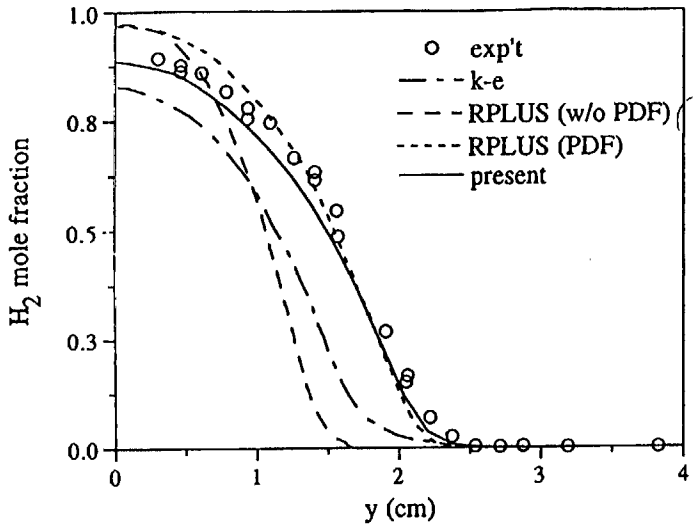
1.0
0.8
0.5
0.3
0.0
0
1
2
3
4
y (cm)
H_2 mole fraction
exp't
k-e
RPLUS (w/o PDF)
RPLUS (PDF)
present

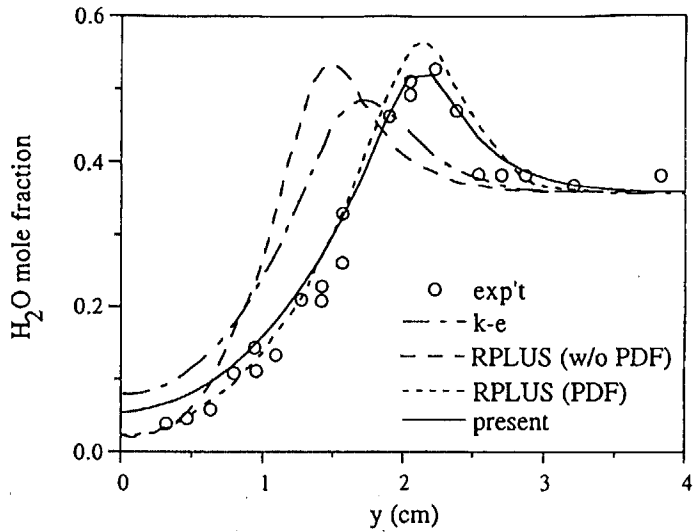
0.6
0.4
0.2
0.0
0
1
2
3
4
y (cm)
H_2O mole fraction
exp't
k-e
RPLUS (w/o PDF)
RPLUS (PDF)
present

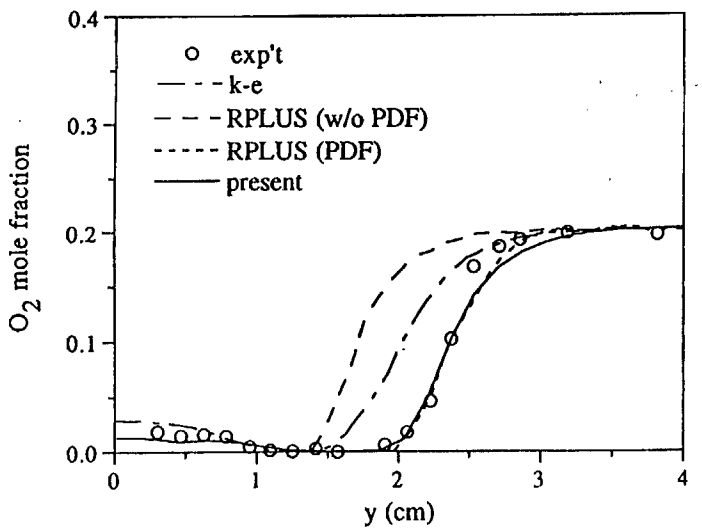
0.4
0.3
0.2
0.1
0.0
0
1
2
3
4
y (cm)
O_2 mole fraction
exp't
k-e
RPLUS (w/o PDF)
RPLUS (PDF)
present

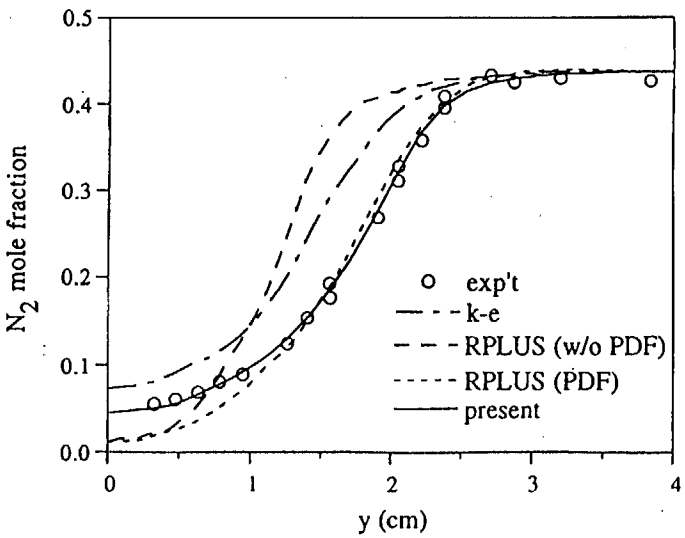
0.5
0.4
0.3
0.2
0.1
0.0
0
1
2
3
4
y (cm)
N_2 mole fraction
exp't
k-e
RPLUS (w/o PDF)
RPLUS (PDF)
present

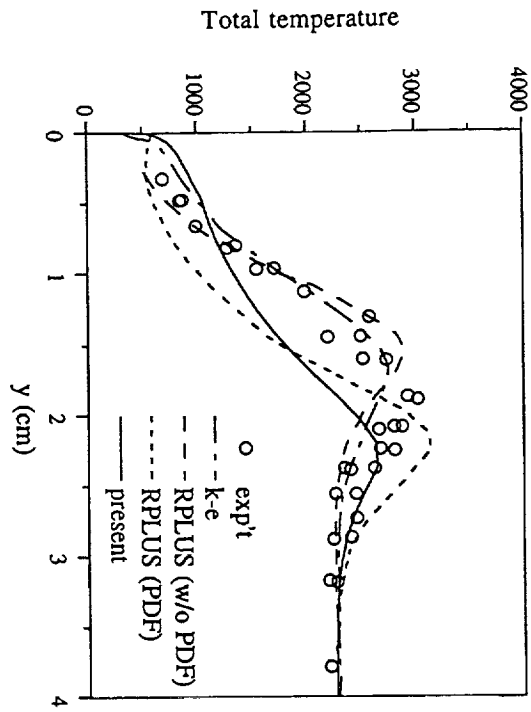

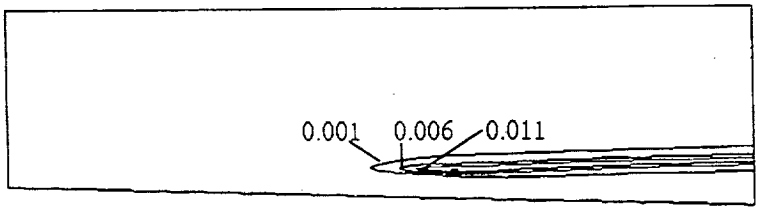

Calculated OH contour.

The numerical result obtained using the M-S turbulence equations indicates that the combustion occurs at approximately middle of the channel. The calculated flame location is in excellent agreement with that observed in the experiment.

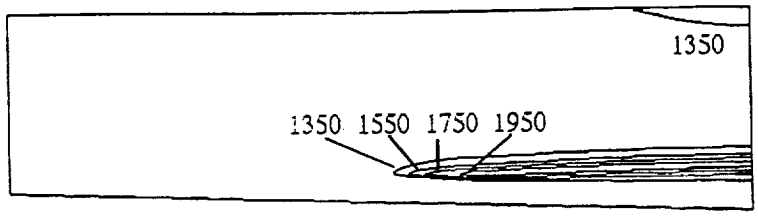

Temperature contours obtained using the M-S turbulence equations

It can be seen in the temperature contours that the calculated flame location obtained using the M-S turbulence equations are in correct agreement with the measured data. The contours also indicate that the temperature increases within in a short distance. The trend is in correct agreement with experimental observations that temperature increase occurs within a finite flame thickness.

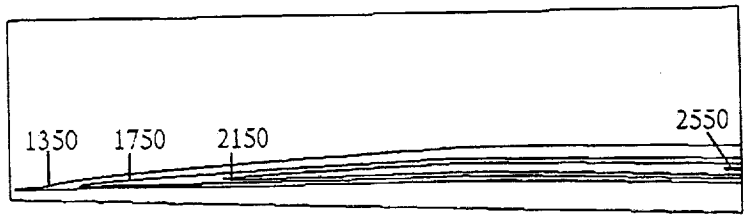

Temperature contours obtained using the pdf*

The pdf fails to predict the correct flame location (i.e., ignition delay). The slowly increasing temperature field indicates that the pdf may not be able to predict a correct flame front. The numerical results obtained using the pdf are not in correct agreement with the physics of combustion.

* A. T. Hsu, Y.-L.P. Tsai, and M. S. Raju, "A PDF approach for compressible turbulent reacting flows," AIAA Paper 93-0087, 1993.

Conclusions and Discussion

The calculated species concentration profiles are in as good agreement with the measured data as those obtained using the pdf.

The flame location (ignition delay) obtained using the multiple-time-scale turb ulence equations is in excellent agreement with the experimentally observed onset of ultraviolet radiation.

Cascade of the turbulence filed is influenced by the extra strains caused by chemical reaction.

Both the numerical results and the measured data exhibit enhanced mixing of the hydrogen and vitiated airstream for the reacting case.

The M-S turbulence equations can resolve the chemical reaction-turbulence interaction.

The pdf produces slowly increasing temperature field and it fails to predict the ignition delay. Thus the numerical results obtained using the pdf are not in correct agreement with physics of combustion.

Part B. Unsteady Transitional Flows over Forced Oscillatory Surfaces*

Contents

* S.-W. Kim, K.B.M.Q. Zaman, and J. Panda, "Calculation of unsteady transitional flow over oscillating airfoil" in *Separated Flows*, eds. J.C. Dutton and L.P. Purtell, Proceeding of ASME Fluid Engineering Conference, Washington D.C., June 20-24, 1993.

Nomenclature

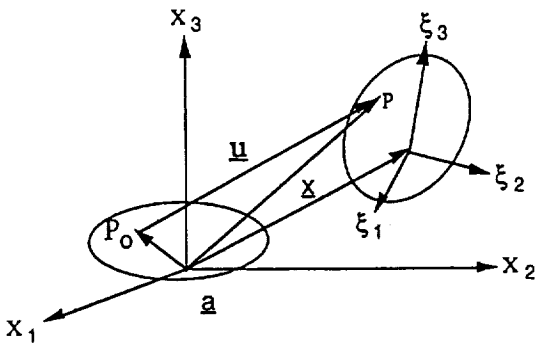

Lagrangian-Eulerian coordinates

x: fixed reference coordinates
ξ: moving coordinates
$J = |\partial \xi_j / \partial a_j|$

Unsteady transitional flow equations with moving boundaries

Conservation of mass equation

$$\frac{\partial}{\partial t}(\rho J) = J\frac{\partial}{\partial x_j}\left\{\rho\left(u_j^g - u_j\right)\right\} \quad (1)$$

Conservation of linear momentum equation

$$\frac{\partial}{\partial t}(\rho u_i J) = J\frac{\partial}{\partial x_j}\left\{\rho u_i\left(u_j^g - u_j\right)\right\} + J\frac{\partial \tau_{ij}}{\partial x_j} - J\frac{\partial p}{\partial x_i} \quad (2)$$

Convection-diffusion equation for scalar variables (i.e., $\phi = \{k_p, \varepsilon_p, k_t, \varepsilon_t,$ etc. $\}$

$$\frac{\partial}{\partial t}(\rho \phi J) = J\frac{\partial}{\partial x_j}\left\{\rho\phi\left(u_j^g - u_j\right)\right\} + J\left\{\mu_e\frac{\partial \phi}{\partial x_j}\right\} - J\rho f(\phi)$$

Numerical Method

The unsteady transitional flow equations are solved using the same finite volume method. Time-integration is made using an iterative-time-advancing scheme.

Comparison of Unsteady Flow Solution Techniques*

Iterative Time-Advancing Scheme (ITA).
Simplified Marker and Cell (SMAC).
Pressure-Implicit Splitting of Operators (PISO).

The ITA that can best resolve the nonlinearity of the Navier-Stokes equations, and yields the most accurate results.

The SMAC is the most efficient computationally and yields accurate numerical results for laminar flows.

The PISO is the most unstable numericaly and yields less accurate results.

* Kim & Benson, Computers and Fluids, vol. 21, pp. 435-454, 1992

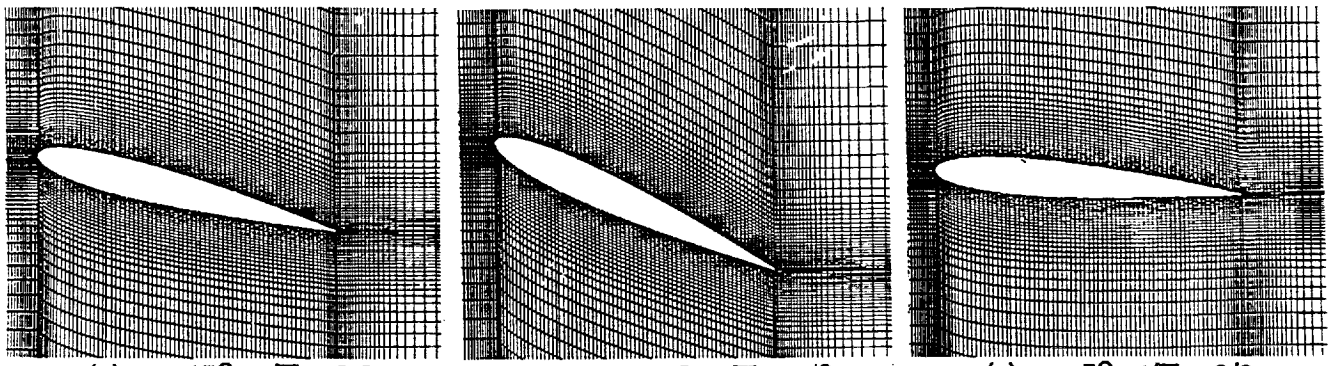

(a) $\alpha = 15^{o}$, $t/T = 0.0$ (b) $\alpha = 25^{o}$, $t/T = \pi/2$ (c) $\alpha = 5^{o}$, $t/T = 3/2\ \pi$

Oscillating airfoil and moving mesh

Comparison of calculated streaklines with smoke picture.

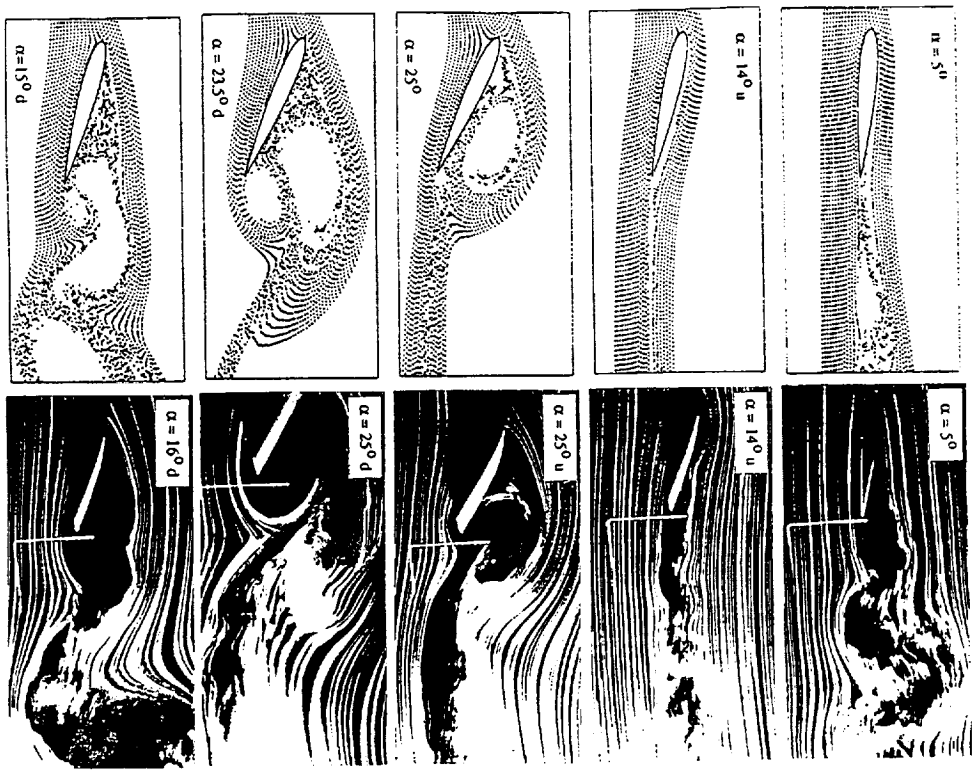

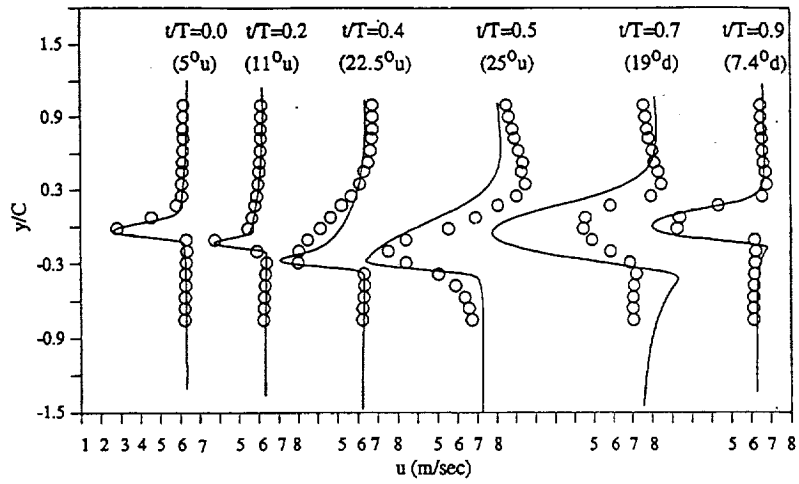

Ensenble-averaged velocity profiles at x/c=1.0

The deteriorated comparison at $\alpha \approx 19^{o}$d

(i) The hot wire can not accurately measure the velocity components when the flow is misaligned more than approximately 30^{o} from the hot wire axis.

(ii) The interaction between the DSV and the TEV occurs in a relatively coarse mesh region and the numerical method yields somewhat deteriorated results.

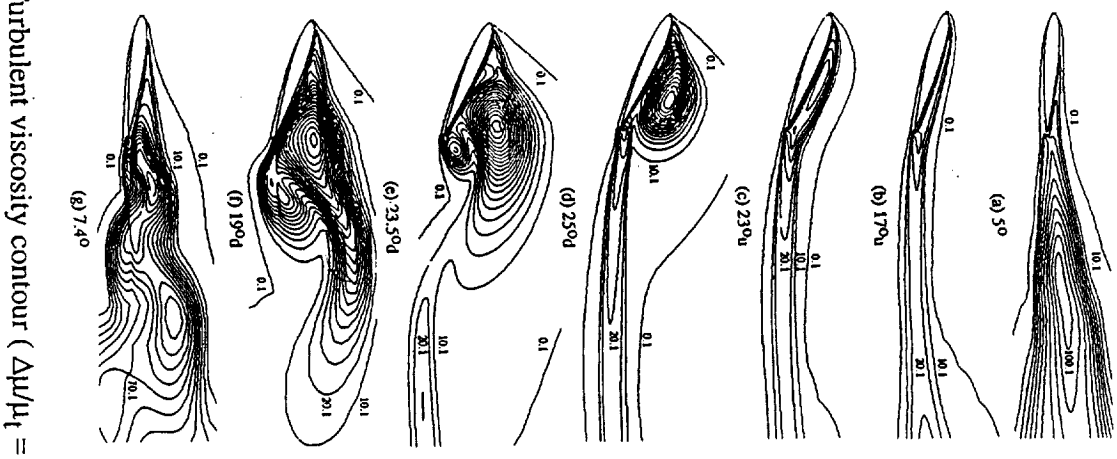

Turbulent viscosity contour ($\Delta\mu/\mu_t = 10$)

CONCLUSIONS AND DISCUSSION

Numerical method successfully predicts the Dynamic Stall Vortex and the Trailing Edge Vortex.

The calculated ensemble-averaged velocity profiles are in good agreement with the measured data.

Both the numerical results and the measured data show that the transition from laminar to turbulent state and relaminarization occur widely in space and in time.

The good comparison between the numerical results and the experimental data are attributed to the capability of

(i) the ITA that can best resolve the nonlinearity of the Navier-Stokes equations,

(ii) the new pressure correction algorithm that can strongly enforce the conservation of mass, and

(iii) the Multiple-time-scale turbulence equations that can resolve the transitional nonequilibrium turbulence field.